AN ABSTRACT OF THE THESIS OF

CHARLES EDWARD STUART JR. (Name) for the MASTER OF SCIENCE (Degree)

in Nuclear Engineering (Major) presented on July 15, 1970 (Date)

Title: A MATHEMATICAL MODEL FOR CAPILLARY GAS CHROMATOGRAPHY

Redacted for privacy

Abstract approved: Dr. Lamar Bupp

In the study of gas chromatography a model is presented to simulate a capillary gas chromatographic system. The model was developed to study the concentrations of sample gas as a function of time and space as it travels through the capillary column. The molecular migration was approximated by elementary diffusion theory and the adsorption processes were described with Langmuir theory. A computer code was written to solve numerically the two coupled differential equations derived for the model.

A commercial gas chromatograph fitted with a capillary column, was used for aquisition of data. The experimental system consisted of a translucent teflon tubing, .0381 cm I. D., as the capillary column. Boron trifluoride was used as the sample gas and argon was used as the carrier gas.

The computer code based upon the derived model was used to

evaluate the diffusion coefficient, mean adsorption time, and the probability of adsorption from experimental data. Reasonable correlations were obtained.

A Mathematical Model for Capillary Gas Chromatography

by

Charles Edward Stuart Jr.

A THESIS

submitted to

Oregon State University

in partial fulfillment of
the requirements for the
degree of

Master of Science

June 1971

APPROVED:

Redacted for privacy

Professor of Nuclear Engineering
in charge of major

Redacted for privacy

Acting Head of Department of Mechanical and Nuclear Engineering

Redacted for privacy

Dean of Graduate School

Date thesis is presented July 15, 1970

Typed by Nancy Kerley for Charles Edward Stuart Jr.

ACKNOWLEDGMENT

The author wishes to express his thanks to Dr. Lamar Bupp for his guidance and moral support throughout the project leading to this thesis; to Dr. D. J. Reed for the use of his lab's gas chromatograph; to the Oregon State Computer Center for their unsupported research grant.

Special thanks to my wife, Susan, for her understanding and help in typing the preliminary copies of this thesis.

TABLE OF CONTENTS

LIST OF TABLES

LIST OF FIGURES

A MATHEMATICAL MODEL FOR CAPILLARY GAS CHROMATOGRAPHY

I. INTRODUCTION

Chromatography has been a versatile analytical tool for many years in the separation of very closely related substances or compounds. Chromatography now involves several different methods, gas chromatography, liquid chromatography, and paper chromatography. The simplest, from an analytical view point, is the subdivision of gas chromatography referred to as capillary gas chromatography. The essential part of gas chromatography is a column, which in capillary chromatography consists of capillary-like tubing, i.e. inside tube diameters of .5 mm or less. The gas chromatographic columns, other than capillary columns, are usually packed columns. In these columns material of high surface-to-volume ratios is packed in the column loosely and gas is forced to flow through the column. In either type of column a gas, referred to as the carrier gas, flows continuously and is the media in which a sample gas is injected. The sample gas concentration profile, as a function of position in the column or time, after it is injected, closely resembles a step function. As the sample gas flows through the column surrounded by the carrier gas, it diffuses into the surrounding carrier gas. With the proper selection of column material, the sample gas will be adsorbed and desorbed on the available surface in the system.

The adsorption-desorption process has the effect of holding up the gas sample with respect to the carrier gas and is referred to as sample retention. This retention is dependent on the chemical nature of the sample gas. The separation of the basic components in a mixture of substances is the result of each component's different chemical nature and thus its different retention time.

Objectives

The objectives of this study of gas chromatography were to determine the essential characteristics of capillary gas chromatography. In doing this a mathematical model describing a capillary chromatographic system was developed. An analytical model that could predict sample gas concentration profiles would have several uses. First, such a model could be used to pin-point the effects on the sample gas profiles of the physical constants associated with the mathematical description of the system. With experimental data, the physical constants associated with the adsorption-desorption process of the system can be found. The diffusion coefficient of the binary sample-carrier gas system can be found with experimental data, also. With the evaluation of the physical constants of a system, the mathematical model could be used to locate optimum system variables.

An essential part of the objectives of this study was to determine

the general effects of each physical constant on the sample-carrier gas system.

II. THEORY

Background

Much of the theoretical work in the past has been done either on a semi-empirical basis or one with which results are obtained after several restrictive assumptions have been made. A common starting point of chromatographic theory is the case of ideal chromatography. The simplifying assumptions are: (a) uniform column, uniformly packed, constant temperature, (b) non-compressible fluid, no changes in fluid volume as the result of adsorption and desorption, the average fluid velocity is the same for all cross sections, (c) no diffusion in an axial direction, and (d) instantaneous and complete equilibrium in any column cross section (14). The original treatment of the theory of ideal chromatography was done by Wilson (28), DeVault (10), and Weiss (27). The restrictions of ideal chromatography severely limits its usefulness in gas chromatography. To make the results of ideal chromatography more useful, workers in the field have introduced correction factors. James and Martin (18) developed a correction term to allow non-compressible fluid theory to be applied to compressible fluids, e.g. carrier gases. Corrections for the effects of the process of adsorption-desorption was made by Bosanquet (4) and others (20). The diffusion has consistantly been related to a theoretical plate height, which includes other effects besides diffusion. In earlier work

(22) more emphasis was given to this theoretical plate height, which now is considered merely a measure of relative spreading of the sample gas in the column, i. e. the broadening of the sample gas packet.

In the following development nearly all of the limitations of ideal chromatography theory will be removed.

Development

When a carrier gas flows through a gas chromatographic column the gas sample diffuses into the carrier gas and is adsorbed and desorbed on the surfaces of the column. For a simple capillary column the surface of the column is the area of the column's walls while in a packed column, the surface area consists of the area of the packing material plus the tube walls. Besides having a very complicated surface area, which may not be constant per unit length of column, diffusion is difficult to describe because of gas flow irregularities and preferential flow passages. The irregularities are caused by non-uniform packing of the column. Because of the irregularities, the development of a model describing packed columns is difficult. The modeling of capillary columns does not have the inherent difficulties of modeling packed columns. A uniform tube has fixed surface characteristics and gas flow through it will be relatively constant.

In Table 1 the notation, constants and variables are defined and

and their units given.

Table 1. Definition of terms.

Term	Units	Definition
N	cm^{-1}	Molecules of gas per centimeter of tubing
C	cm^{-1}	Molecules of gas on tubing walls per cm
Σ	sec^{-1}	Probability of adsorption per second
τ	sec	Mean life time of molecules on tubing walls
D	cm^2/sec	Diffusion coefficient
v	cm/sec	Mean molecular gas velocity
V	cm/sec	Bulk gas velocity with respect to column
$\bar{\nabla}$	cm^{-1}	Gradient operator
x	cm	Variable in axial dimension
λ	sec^{-1}	Inverse of mean life, $\frac{1}{\tau}$
Z	$1/(cm^2\text{-sec})$	Collision of gas molecules with wall per unit area per second
Mw	amu	Molecular weight

Consider a control volume, $\Delta x \Delta y \Delta x$, which is moving with the gas flow which contains a sample gas A. The conservation of mass for the control volume is:

$$\left\{\begin{array}{l}\text{Net rate of}\\ \text{mass A out}\\ \text{of control}\\ \text{volume}\end{array}\right\} = -\left\{\begin{array}{l}\text{Net rate of}\\ \text{leakage out}\\ \text{of control}\\ \text{volume}\end{array}\right\} - \left\{\begin{array}{l}\text{Rate of}\\ \text{adsorption}\\ \text{onto capillary}\\ \text{walls}\end{array}\right\} + \left\{\begin{array}{l}\text{Rate of}\\ \text{desorption}\\ \text{from capillary}\\ \text{walls}\end{array}\right\}$$

Now let N be the number of molecules of gas A per unit length of tubing. Then the time rate of change of N is:

$$\frac{\partial N(r, t)}{\partial t} .$$

The leakage from the control volume is exactly:

$$-\bar{\nabla} \cdot \bar{J}(\bar{r}, t)$$

where $\bar{J}(\bar{r}, t)$ is the net flow of gas A molecules at point $\bar{r}$, i. e. the net molecular current. The diffusion theory approximation to the problem of moleculear migration gives:

$$\bar{J}(\bar{r}, t) = -D\bar{\nabla} N,$$

where D is referred to as the diffusion coefficient, this is commonly called Fick's first law. The leakage is now:

$$\bar{\nabla} \cdot D\bar{\nabla} N(\bar{r}, t) .$$

The net rate of adsorption will be proportional to the density, N, with the probability of adsorption per second is given by $\Sigma(\bar{r})$. The rate of adsorption is:

$$-\Sigma(\bar{r}, t) N(\bar{r}, t) .$$

The desorption from the capillary walls is given by:

$$+\frac{C(x, t)}{\tau}$$

where $C(x, t)$ is the number of molecules of gas A on the capillary

walls per unit length and τ is the mean time each molecule spends on the walls.

Now the analytical equation of conservation of mass is:

$$\frac{\partial}{\partial t} N(\bar{r}, t) = \bar{\nabla} \cdot D(\bar{r}, t)\, \bar{\nabla} N(\bar{r}, t) - \Sigma(\bar{r}, t)\, N(\bar{r}, t) + \frac{C(x, t)}{\tau(x, t)} \qquad (1)$$

The conservation of mass for the capillary walls is:

$$\left\{\begin{array}{l}\text{Net rate of}\\ \text{molecules leaving}\\ \text{capillary walls}\end{array}\right\} = - \left\{\begin{array}{l}\text{Rate of}\\ \text{adsorption}\\ \text{onto walls}\end{array}\right\} + \left\{\begin{array}{l}\text{Rate of}\\ \text{desorption}\\ \text{from walls}\end{array}\right\}$$

From preceeding analysis the analytical form is:

$$\frac{\partial C(x, t)}{\partial t} = \Sigma N(x, t) - \frac{C(x, t)}{\tau(x, t)} \quad . \qquad (2)$$

Note that nothing has been stated about the spatial and time dependence of the constants.

The analysis will now be restricted to one-dimension, x, this eliminates much of the complications of the gradient operators, $\bar{\nabla}$. By restricting the analysis to one-dimension, the assumption is implied that the concentration, N, is constant in the radial direction. This would be true in the simplest case for mixed gas flow except near the capillary walls where the density, N, is somewhat smaller because of adsorption on the walls.

The adsorption term will for now be simply referred to as the adsorption probability, Σ, times $N(x, t)$. Later the adsorption

probability will be discussed in more detail. The mean residence time, τ, will be assumed constant.

To this point the fact that the gas is moving with respect to the capillary walls has been ignored. Let x be the coordinate fixed to the capillary walls and x' be fixed to the flowing gas in the capillary tubing, shown in Figure 1.

$x' = x - V \cdot t$

$x = x' + V \cdot t$

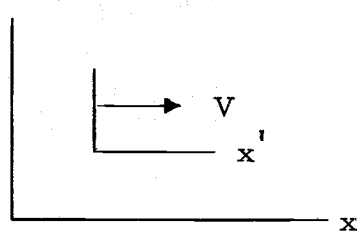

V is the gas velocity fixed with respect to the capillary walls.

Figure 1. Coordinate system.

Now the two time-dependent equations that describe the system are:

$$\frac{\partial N(x', t)}{\partial t} = \frac{\partial}{\partial x} D(x', t) \frac{\partial}{\partial x} N(x', t) - \Sigma(x') N(x', t) + \frac{C(x+vt)}{\tau} \qquad (3)$$

and

$$\frac{\partial}{\partial t} C(x, t) = \Sigma N(x' - vt) - \frac{C(x, t)}{\tau} . \qquad (4)$$

From this point on let $N(x, t)$ and $C(x, t)$ be the number of molecules of gas A per centimeter of tubing and $n(x, t)$ is the molecular density of gas A.

There are two types of adsorption that are of importance here: physical and chemical. In physical adsorption there exists an

attractive force between the solid surface of the tube walls and the mobile gas molecule. Chemical adsorption or chemisorption occurs when an actual chemical bond is formed between the gas molecule and the solid surface. Physical adsorption may be characterized by two types of behavior, the first being the forming of a monomolecular layer on the surface which is different in character than subsequent adsorption. The second is the formation of multilayers of molecules by condensation. Langmuir's theory (21) is concerned with the formation of monomolecular layers and limits adsorption to the monomolecular layers. The theory of multimolecular layers is called BET theory (6) after its founders, Bruanauer, Emmett and Teller, and produces good results when compared to experimental data. Figure 2 shows isotherms predicted by both Langmuir and the BET theory.

Both Langmuir and BET theory agree up to the pressure P_1. At this pressure the first molecular layer has been completed and multilayer formation is becoming important. For operating pressure up to P_1 the use of Langmuir theory is justified.

When chemisorption occurs the simple Langmuir theory is more applicable than BET theory. This is because the surface area available to the gas for chemical interaction with the surface is proportional to the rate of chemisorption, i. e. the formation of a monomolecular layer of chemisorbed molecules.

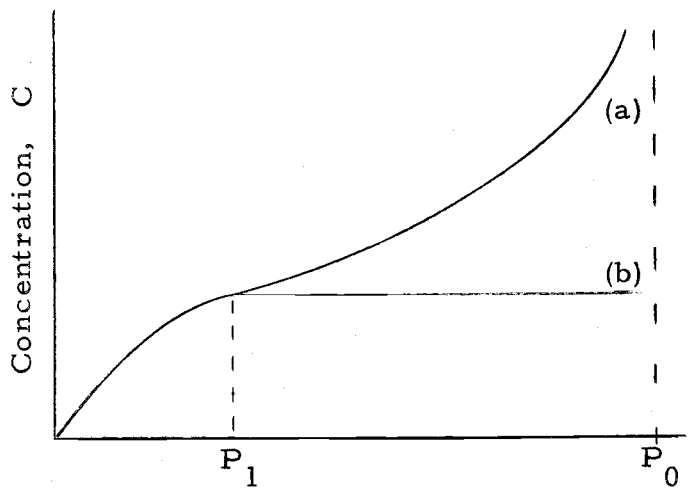

Figure 2. Concentration of adsorbed gas molecules versus pressure for BET and Langmuir isotherms.

The adsorption time, τ, is on the order of molecular vibration frequency, 10^{-12} sec, when there exists no attraction forces between the gas molecule and the solid surface. The other extreme is when permanent chemisorption occurs and the adsorption time may approach infinity. When attractive forces are present, Frenkel (11) proposed the following equation for the adsorption time, τ:

$$\tau = \tau_0 \exp\left(\frac{Q}{RT}\right) \tag{5}$$

Where Q is the adsorption energy, i.e. heat of adsorption, and R is the universal gas constant. The value of τ_0 is that of the molecular vibration frequency, 10^{-12} sec (11). If the value of τ is an order of magnitude or larger than τ_0, it would be safe to say

that adsorption has occurred. Table 2 shows the adsorption time as a function of Q. The accommodation coefficient, z, in Table 2 is what Adamson (1) defines as the probability of adsorption of a gas molecule per collision with the solid surface. The surface concentration in Table 2 was calculated by:

$$C = Zrz \tag{6}$$

Where Z is the number of collisions per second expressed in compatible units for the surface concentration, C. The accommodation coefficient, z, was assumed to be unity, i. e. each molecule that strikes the surface is adsorbed. The values of C calculated in this way are excessively large for values of τ, corresponding to chemisorption, and are thus meaningless. For small values of adsorption times and/or small values of the accommodation coefficient, equation (6) gives fair results. Thus, requirement for validity of equation (6) for small values of C will be used as a check on the consistency of a more complicated model relating adsorption time and surface concentration.

The adsorption time can be considered a constant for any isotherm case. This may not be strictly true if the adsorption energy, Q, is influenced by adjacent adsorbed molecules. This will only occur when a complete monomolecular layer is being approached. Any effect on the adsorption time for adjacent adsorbed molecules will be ignored.

Table 2. The adsorption spectrum (1).

Q kcal/mole	τ, sec 20°C	C, net moles/cm	Comments
.1	10^{-13}	9	Adsorption nill; specular reflections; accommodation coefficient zero
1.5	10^{-12}	0	Region of physical adsorption; accommodation coefficient unity
3.5	4×10^{-11}	10^{-12}	
3.9	4×10^{-7}	10^{-8}	
20.0	100		Region of chemisorption
40.0	10^{17}		

The derivation of an expression for the probability of adsorption from Langmuir theory assumed the surfaces are uniform, only a monomolecular layer forms, and that there is no attractive forces between adsorbed molecules. Then the rate of adsorption, ΣN, is proportional to the unoccupied surface area, $S_0 - S_1$, (S_0 is the total surface area and S_1 is the covered surface area). If C_0 is the maximum concentration of molecules on the surface then:

$$S_0 - S_1 \propto (1 - \frac{C}{C_0})$$

and

$$\Sigma = A(1 - \frac{C}{C_0})$$

Where A is the proportionality constant. The rate of adsorption is also proportional to the number of collisions occurring per second per unit area, A. Let A be the product of a constant P_0 and Z.

Then:

$$\Sigma N = ZP_0(1 - \frac{C}{C_0}) \tag{7}$$

The constant P_0 is clearly the probability that one molecule will have a collision with the surface and be adsorbed per unit length of tubing. Now the rate equation for the concentration of molecules on the surface is:

$$\frac{dC(t)}{dt} = ZP_0(1 - \frac{C(t)}{C_0}) - \frac{C(t)}{\tau} \tag{8}$$

The equilibrium concentration on C is:

$$C_\infty = \frac{P_0 \tau Z}{1 + \frac{Z \tau P_0}{C_0}} \tag{9}$$

Recall that for consistency, equation (6) should hold for small surface concentrations. If $P_0 Z$ is small compared to one, i.e. $\frac{Z\tau P_0}{C_0} \ll 1$, then equation (9) reduces to:

$$C_\infty = P_0 \tau Z \tag{10}$$

If P_0 is unity then equation (10) reduces to equation (6). If on the other hand the term is much larger than one the surface concentration is C_0, the maximum concentration, as it should be.

The number of collisions that occurs per second per unit area, Z, is calculated by elementary gas kinetics with the results that:

$$Z = \frac{1}{2} vn \tag{11}$$

Where v is the average molecular velocity and n is the molecular density. Solving the integral transport equation (see Appendix A), taking into account the geometry factors it was found that:

$$Z = vn \frac{\left(\frac{\pi}{2} - \phi(R)\right)}{\pi} \tag{12}$$

The function $\phi(R)$ is dependent on the tube radius, R, and the mean free path of the gas. The collision per second per unit area is well approximated by the equation (11) for tubing with a diameter even much smaller than .001 cm.

The adsorption coefficient, Σ, can be found by expanding equation (7), recalling that n, molecules per cm^3, is related to N, molecules per cm of tubing, by a factor of $\frac{1}{\pi R^2}$, R tube radius.

$$\Sigma = \frac{vP_0}{2\pi R^2} \left(1 - \frac{C}{C_0}\right) \quad \text{or} \quad \Sigma = \Sigma_0 v \left(1 - \frac{C}{C_0}\right) \tag{13}$$

where

$$\Sigma_0 = \frac{P_0}{2\pi R^2} \tag{14}$$

The average molecular velocity is calculated from (23):

$$v = \left(\frac{8kT}{\pi m}\right)^{\frac{1}{2}} \quad \text{or} \quad v = 1.455 \times 10^4 \left(\frac{T}{Mw}\right)^{\frac{1}{2}} \tag{15}$$

Where T is the temperature, K is Boltzman constant, m is mass of the molecule, and Mw its molecular weight.

Summary

In the development of the model several added assumptions were made in place of the assumption's of ideal chromatography that were removed. The added assumptions are: (a) Langmuir adsorption is valid in the pressure ranges under consideration, and (b) there is no interaction between adsorbed molecules, thus the mean adsorption time is constant. The restriction of ideal gas chromatography theory that have been retained are: (a) uniform column, constant temperature, and (b) non-compressible fluid. The retained restrictions are less restrictive for capillary columns than packed columns, because capillary columns are inherently more uniform and pressure gradients are smaller for the same flow rate in capillary columns than in packed columns. Axial diffusion and non-equilibrium conditions are now allowed.

III. GAS CHROMATOGRAPHIC SYSTEM

A gas chromatograph consisted of two major systems; the gas flow system and the gas detector. Each of these systems had several subsystems that were essential to operation. A F & M, 810 Series Research Chromatography with a dual flame gas detector was used.

The gas flow system consisted of two separate systems; the carrier gas and the hydrogen combustion gas system. The carrier gas flow system is shown in Figure 3. The carrier gas flow rate, for each system, was continuously monitored in rotometers and controlled by needle valves, which were located immediately down stream of the rotometers. At the injection port the gas sample was injected into the carrier gas flow, with a syringe through a rubber septum, just before the carrier gas entered the column. The injection port is shown in Figure 4.

The hydrogen gas for the detector flowed from the compressed gas tank through a needle valve and then into the detector where it was mixed with the carrier and sample gases. In the detector the hydrogen gas was burned in the presence of the columns effluent, i.e. carrier and sample gas. The sample gas was burned and ionized in the detector flame. When a positive potential was placed on the collector ring, Figure 5, the electrons were collected to produce a current. This current flowed through an input resistor, between 10^{11} and 10^{6}

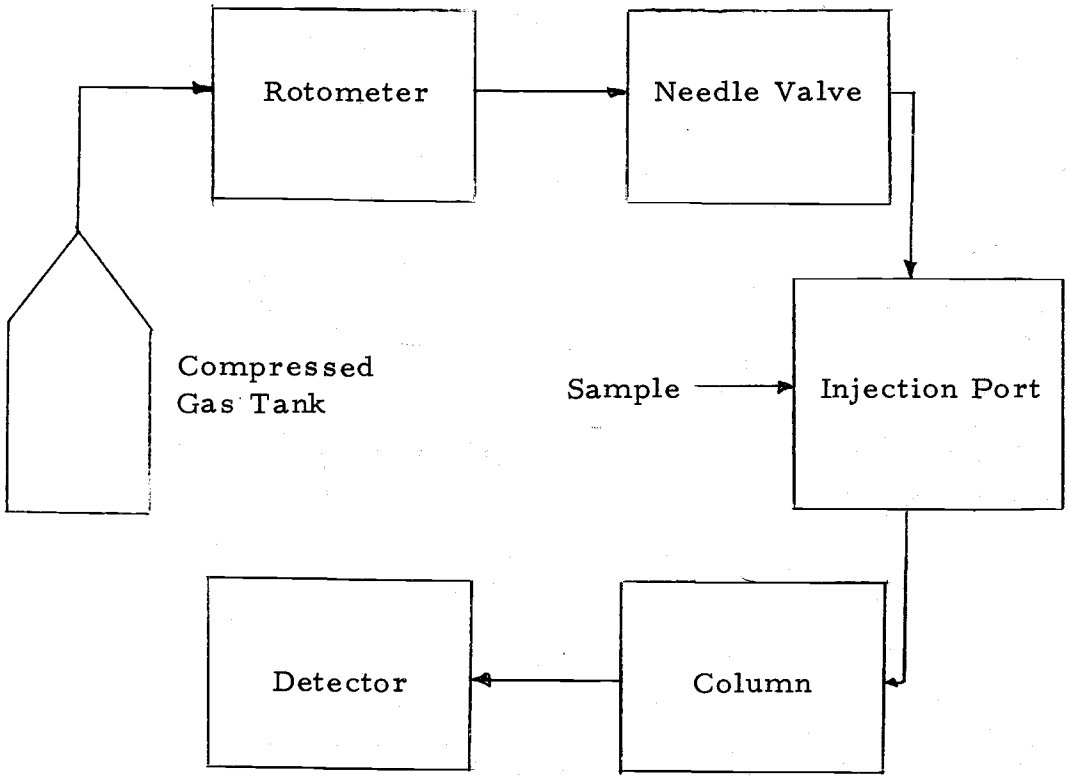

Figure 3. Carrier gas flow.

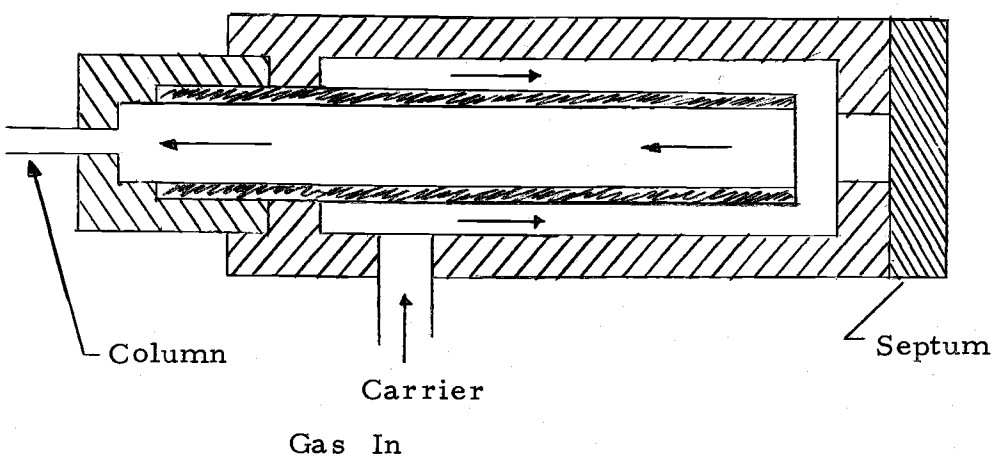

Figure 4. Simplified cross section view of injection port.

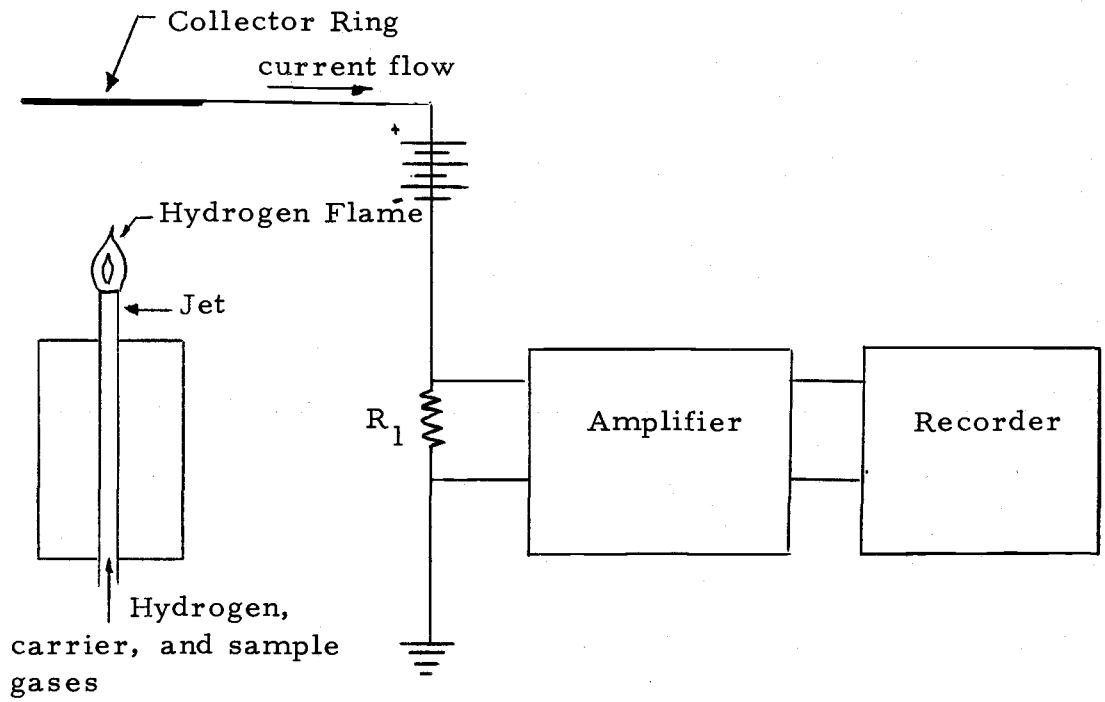

Figure 5. Hydrogen flame detector system.

ohms, producing an output voltage that was amplified and recorded. The input resistor was varied by means of a Range switch on the control panel and had five positions: 10^4, 10^3, 10^2, 10 and 1. The smallest Range setting, one, was the most sensitive and the largest, 10^4, was the least sensitive. The signal to the recorder, a Honeywell Class 15 recorder, which had a maximum input voltage of 10 millivolts, could be attenuated by any multiple of two up to 256, e.g. 1, 2, 4, 8, 16, etc.

The chromatograph system was a dual column system. There were two detectors, two injection ports, and two carrier gas flow

systems. The dual carrier gas systems operated at the same pressure but had separate needle valves to control the flow. The signal to the amplifier and recorder could originate from either detector separately or as the difference of the two detector outputs for dual column operation.

The capillary column was located in an oven, which could be heated to 200° C. The column was transluent teflon tubing with an inside diameter of .0381 cm. The teflon tubing was used because of its stability at temperatures up to 250° C and its chemical inertness.

Boron trifluoride was used as the sample gas and argon as the carrier gas. Boron trifluoride was used because of its availability, gaseous state, and stability. There also existed the possibility that the boron trifluoride might produce some bond, either physical or chemical, with the teflon tubing, the boron trifluoride reservoir was constructed so that the syringe could be filled, by means of a septum placed in a brass tee fitting, as shown in Figure 6.

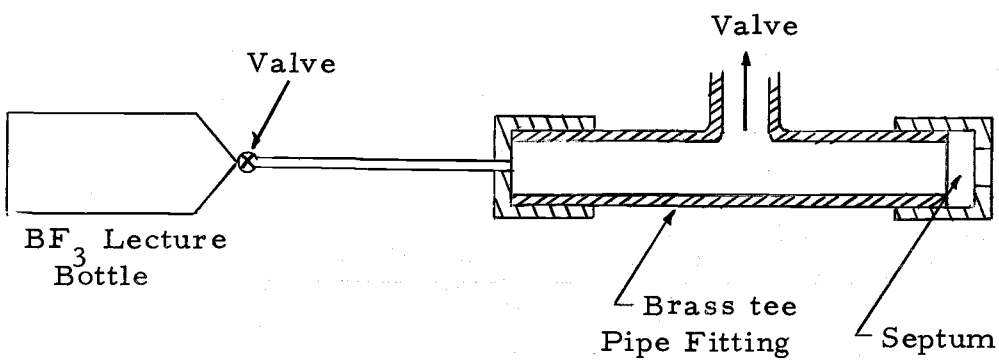

Figure 6. Boron trifluoride reservoir.

IV. EXPERIMENTAL PROCEDURE

The F & M gas chromatograph was used in the single column mode of operation. The "B" detector and gas system were used. The "A" detector was extremely noisy when the sensitivity was in the needed range, ten. With one detector being too noisy, the use of the gas chromatograph in the dual column mode was ruled out. The temperature control was only used when data were taken at temperatures higher than room temperature, at which temperature most data were taken.

The first step in starting the gas chromatograph was to initiate the carrier gas flow. This was done by opening the valve at the pressure regulator on the compressed gas tank. The desired pressure, 20 psig, was set by the pressure regulator at the tank. The closing of the needle valve controlling the flow of A carrier gas system, resulted in a very small total flow rate and a long wait for the pressure to stabilize. By allowing gas to flow continuously through the A system and into the atmosphere the pressure stabilized very quickly. The next step was to turn on the hydrogen gas flow, which was regulated to five psig by the hydrogen tank regulator. With the hydrogen gas flowing it was then ignited by pressing the manual ignite button. With this done, the hydrogen flame detector electronics was switched from off to the warm up mode and it then remained in this mode for

15 minutes. After the 15 minute warm up period the mode was switched from warm up to flame and the detector-amplifier system was ready. During the warm up period the recorder was turned on so that it would be warmed up when the detector electronics was ready.

Each sequence of runs was controlled to produce the same shape or profile of the gas packet after traveling through the capillary tubing for different lengths of time. Two methods were tried to accomplish this; in the first the column was of a fixed length and the flow rate was varied. This produced very poor results because the packet shape was too dependent on the flow rate, i.e. the rate of which the sample entered the column in the injection port. The difference in profile as a function of flow rate occurred because a given volume of sample when injected into the port does not instantaneously enter the column. The time period for the sample to completely enter the column depended directly on the volumetric flow rate. Each flow rate produced different flow patterns entering the column and thus different initial profiles. The second and more successful method was to maintain, as close as possible, the same flow rate and vary the length of the column. This resulted in packet profiles that were dependent only on the length of time they were in the column and their velocity while in the column.

The procedure for each run consisted of initially adjusting the

attenuation so that the signal to the recorder was under 10 millivolts. This was only needed several times during a sequence of runs. With the desired length of column in place, the sample was placed in the syringe at the boron trifluoride reservior and then injected into the carrier gas in the injection port. Each sequence of runs consisted of several runs for 40 and 270 centimeter lengths of tubing. Flow rates were maintained at about .2 ml/sec at discharge from the tubing.

V. ANALYSIS OF DATA

From the experimental data taken from the charts of the gas chromatograph's chart recorder, profiles of the BF_3 gas packets were found. The profiles consisted of sample gas sets that had traveled through column lengths of 40 and 270 cms. The profile corresponding to the 40 cm column was considered the starting point for the 270 cm column. Thus, in the analysis there existed a factious 230 cm column, of which the profile of the sample gas as it entered the column and the profile after it exited from the column was available. In this way the effects of the sample entering the column in the injection port were removed as a system variable. From these profiles the value of the diffusion coefficient, D, the adsorption time, τ, and the adsorption probability, Σ, were determined. To do this a solution to the equations derived in Chapter II was found.

Solution

The equations to be solved, equations (3) and (4), were two non-linear, coupled, spaced and time dependent differential equations.

$$\frac{dN(x,t)}{dt} = \frac{d}{dx} D \frac{d}{dx} N(x,t) - \Sigma N(x,t) + \frac{C(x',t)}{\tau} \qquad (3)$$

$$\frac{dC(x',t)}{dt} = \Sigma N(x,t) - \frac{C(x',t)}{\tau} \qquad (4)$$

The fact that the two coordinate systems x and x' were moving with respect to each other, with velocity, V, made the exact solution to these equations extremely difficult if not impossible. The procedure required to solve these equations numerically was relatively straight forward.

In the numerical solution, the continuous functions in space and time were replaced by discrete points that were separated in space by h_x and in time by h_t. To develop a numerical scheme the differential equations were first integrated with respect to time, from t_0 to t_1. The terms containing the gas density, $N(x, t)$, were assumed to be constant with respect to time for the period t_0 to t_1, where $h_t = t_1 - t_0$. It was assumed that the gas remained fixed with respect to the wall for this time period. The term in equation (3) containing the wall concentration was assumed to be of this form:

$$C(x)\ EXP(-\lambda t)$$

Where λ is the reciprocal of the adsorption time, τ. The value of $C(x)$ was determined by the previous integration or in the case of the first time step by the initial value of $C(x, 0)$. The integral of the complete term in equation (3) is:

$$C(x)(1-EXP(-\lambda h_t))$$

and if the product λh_t is small enough the integral is closely approximated by:

$$+ \lambda C(x)h_t \quad .$$

Which is the same results if we would have assumed $C(x, t)$ to be constant over the interval, h_t. The first form of the integral will be retained. For simplicity let:

$$\lambda^* = \frac{(1-EXP(-\lambda h_t))}{h_t} \tag{16}$$

Let j be the time index and then the two numerical equations are:

$$N_{j+1}(x) = N_j(x) + h_t \left(\frac{d}{dx} D \frac{d}{dx} N_j(x) - \Sigma N_j(x) + \lambda^* C_j(x)\right) \tag{17a}$$

and

$$C_{j+1}(x) = C_j(x) + h_t(\Sigma N_j(x) - \lambda^* C_j(x)) \quad . \tag{17b}$$

These equations have accuracy on the order of $h_t^2 N''$ (15) and if the time step, h_t is taken small enough the solution will converge to the correct answer.

To this point, the division of the space variable into discrete points has been neglected. The term containing the divergence of the current in one dimension and can be approximated using the central difference method. That is:

$$\frac{d^2N(x_i)}{dx^2} \approx \frac{(N_{i+1} - 2N_i + N_{i-1})}{h_x^2}$$

Where i is the space index.

Another way of handling the space dependence would be to

expand the initial profile with a set of analytical functions. The wall concentrations, $C_j(x)$, would also be expanded with a similar, but different, set of functions. These functions could be represented by:

$$N_j(x) = \sum_{i=1}^{N} F_i(x)$$

and

$$C_j(x) = \sum_{i=1}^{M} G_i(x) \quad .$$

In this way equations (13) and (14) need not be solved for each space point at every time step. The profiles would require refitting each time step to the expansion and if an expansion containing only several terms could be found that represent the initial profiles well, refitting should take considerably less effort than solving equations (13) and (14) for each space point.

The set of functions F_i and G_i by no means needs to be orthogonal, even though the curve fitting would be simplified. One of the functions would probably be gaussian in nature to fit the main peak and the other terms representing the non-gaussian nature of the profiles.

The Computer Codes

Two computer codes were written, the first code was to process the data that was taken from the charts, of the chromatograph's chart

recorder, containing the experimental profiles. The processing consisted of converting the chart position into lapsed time, from sample injection to detection, using the gas bulk velocity to convert time to position, normalizing the maximum peak height to 100 and numerically integrating the area under the peak. In addition to this, the code, called DATA PROCESSING, calculated several parameters associated with the shape of the profile. These parameters were the total, leading and trailing widths at one-half and three-fourths the peaks maximum. The leading width was the forward side of gas sample and first to be detected when entering the detector. Figure 7 shows graphically the meaning of the terms.

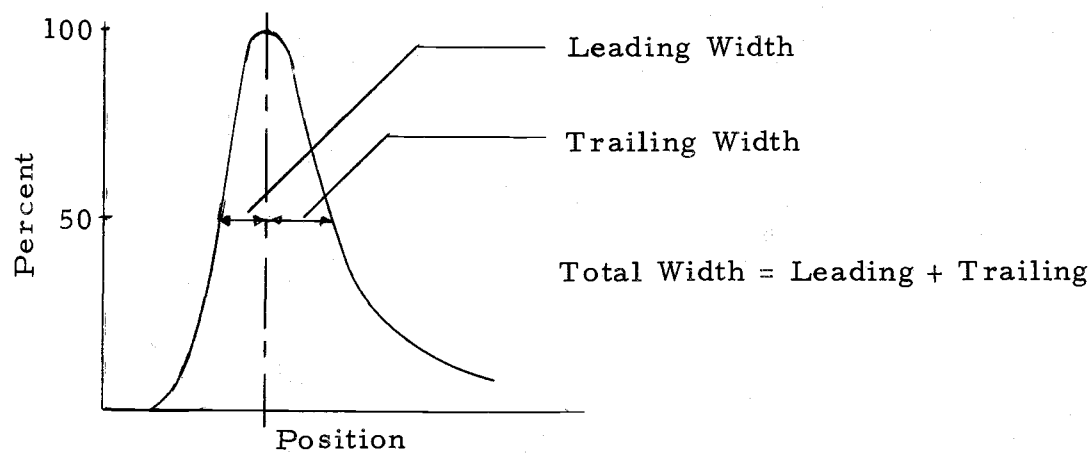

Figure 7. Typical profile. Sample gas concentration versus position.

The second code, titled GAS CHROMATOGRAPHY which will be referred to as GAS, produced the numerical solution to equations (3) and (4). The code was divided into the main calling program and three subroutines, INITIAL, DIFFUSE and SHAPE. The calling

program, GAS, has two functions; the first is to read in the physical constants concerning that run, e.g. diffusion coefficient, adsorption time, adsorption probability, time lapse, etc. The final function is to print out the profile at the end of a run upon request.

In the INITIAL subroutine, the data from the charts were read in and placed in the proper form for the other subroutines to use. In the numerical solution the separation between space points, h_x, is a constant. The data from the charts were usually unevenly spaced and too widely spaced for good numerical accuracy. The initial data, from the charts, were spaced about 2.5 cm and for good numerical accuracy the separation between space points should be about one-half a centimeter. Thus, the initial points were interpolated to convert them to a usable form.

The interpolation method first tried was linear interpolation. This method had the advantage of being very simple and quickly executed. The major disadvantage of linear interpolation was that the central difference approximation to the second derivative of $N(x)$, is zero when the three points used in the approximation were initially found by interpolating between the same two data points. The method finally used for interpolation was a second order Lagrangian method, in which three points were fitted to a second order polynomial. Calculation of the constants for Lagrangian interpolation were more time consuming, but because they need only be calculated

approximately every 5 cm instead of about every 2.5 cm as in the case of linear interpolation, the computer running time was only slightly longer.

In the DIFFUSION subroutine the solution to equations (13) and (14) occurs. The subroutine has two parts, of which only one is executed per run. The solution to the complete set of equations (13) and (14), occurs in the first section and in the case of pure diffusion equation (13) is solved neglecting the terms involving Σ and λ. Doing this reduces the time required for solution of a pure diffusion problem by a factor of one-half when compared to the same solution using the complete set of equations. To this point the fact that the gas is moving with respect to the column has been ignored. During each time step the gas and column are assumed to be fixed relative to each other and at the end of each time step the array corresponding to the wall concentration is shifted one index, i.e. $C_{i,j}$ goes to $C_{i-1,j}$. This approximates the continuous motion of the gas with respect to the column wall with a finite number of jumps, which occur at the end of each h_t seconds. The bulk gas velocity is the ratio of h_x and h_t, so that both h_x and h_t are not independently chosen.

The constants inputted in GAS are not exactly the same as those in Table 1. The mean life or adsorption time is input as λ not τ. The mean molecular velocity, v, has been factored out of both the

diffusion coefficient, D, and the adsorption probability, Σ. The temperature and molecular weight are inputted and the velocity, v, is calculated from equation (13). A zero subscript on D and Σ will refer to values that have had v factored out of them.

An abstract and a copy of the codes DATAPR and GAS are found in Appendix B and C respectively.

Numerical Convergence

To check out the code, GAS, to see if it's numerical scheme would converge to the correct answer, a problem was needed for which an exact solution existed. The problem had to be much simpler than the type the code was written for. The problem chosen was a zero dimensional case with the wall concentration at zero at time zero and the gas density constant. The value for the mean life was chosen at 1 sec and the adsorption probability, Σ_0, at 10^{-7}. A step size of .05 sec was used. The analytical solution agreed to within .0002% of the code's results after four seconds.

The next check on the code was to vary the step sizes of both space and time, and compare the results for uniformity for a typical problem. In doing this a standard set of physical constants and initial profiles were used. The results are shown in Table 3.

Six runs were done with h_t equal to .1, .05 and .025 sec with h_x equal to 1 and .5 cm. Of the six runs four gave very consistant

Table 3. Effect of time and space step sizes.

Width		H_t = .1 sec		H_t = .05 sec		H_t = .025 sec	
	H_x:	.5	1.0	.5	1.0	.05	1.0
		#1	#2	#3	#4	#5	#6
Total	@ 1/2	xxx	24.26	24.23	24.23	27.15	24.22
	3/4	xxx	15.31	15.30	15.30	17.17	15.29
Leading	@ 1/2	xxx	13.73	13.70	13.70	15.06	13.68
	3/4	xxx	8.33	8.31	8.31	9.24	8.30
Trailing	@ 1/2	xxx	10.53	10.54	10.53	12.09	10.54
	3/4	xxx	6.98	6.99	6.99	7.93	6.99
Fixed	$\Sigma_0 = 1.0 \times 10^{-7}$ $D_0 = 5.0 \times 10^{-5}$ $\lambda_0 = 4$			Lapsed time, 9.5 sec			

numbers, one produced values of the widths that were about 20% too large and in one run the numerical scheme was unstable and diverged. The reason the set with h_x and h_t was equal to .5 and .1, respectively, diverged was because for that value of h_x the time step was such that the diffusion term in the equation (17a) was too large. The increase in h_x to 1 cm resulted in a smaller diffusion term with respect to the time step, and numerical convergence. The fifth run with h_x and h_t was equal to .5 cm and .025 cm sec, respectively, which resulted in values of widths that were too large, was the result of bad numerics in the coupling of the two equations or purely in equation (17b). With the proper choice of h_x and h_t the code will converge as can be seen by the less than one percent

difference in the 2, 3, 4, and 6th runs in Table 3.

Shape Dependence

The physical shapes of sample gas concentration are dependent on the diffusion coefficient, mean adsorption time and the probability of adsorption. To study the effect of each parameter on the shape of the gas packet an initial profile was needed. Then all but one parameter was held constant while several runs were made with different values of the parameter under study. Table 4 shows the effect of pure diffusion coefficient, D_0.

Table 4. Pure diffusion.

Width		Diffusion Coefficient, D_0 8.0×10^{-5}	9×10^{-5}	10×10^{-5}	Initial
Total	@ 1/2	26.24 cm	26.94 cm	27.63 cm	19.96 cm
	3/4	16.60	17.05	17.49	12.62
Leading	@ 1/2	11.90	12.16	12.42	8.92
	3/4	7.90	8.02	8.14	6.25
Trailing	@ 1/2	14.34	14.78	15.21	11.04
	3/4	8.71	9.04	9.36	6.36

$\Sigma_0 = 0$

$\tau = 0$, Lapsed time 9.5 sec

The effect of variation of the adsorption time is displayed in Table 5, along with the effect of velocity and the adsorption

probability. The inverse of the adsorption time, λ, is shown in the table. As λ decreases, i.e. τ increases, the leading width increases, the trailing width decreases and the total width decreases. This decrease in the trailing width and increase in the leading width implies that the larger the adsorption time the less the holdup of sample gas by adsorption, just backwards from what might be expected at first glance. It would be expected that the τ equal to the molecular vibrational frequency the shape and widths would remain the same as those of pure diffusion and as τ increased adsorbed molecules would be desorbed somewhat down flow of where they were adsorbed. This would increase the trailing width and decreases the leading width as the desorption time increased. This does occur, but as τ becomes too large the adsorbed molecules are not being desorbed until the gas packet has effectively passed and there seems to be only adsorption as far as the shape of the packet is concerned. Figure 8 shows a sketch of the trailing width as a function of the adsorption time. The behavior of the trailing width is a good indication as to the changing of a packet's shape.

The effect of the adsorption probability shown in Table 5 shows that the holding up of the gas packet, i.e. skewing the packet and sharpening the leading edge (14, 24), is increased with the increasing adsorption. This was to be expected because the adsorption just enhances the effect of the adsorption time in skewing the packet.

Table 5. Effect of λ and Σ_0 on sample packet.

Width		Pure D	λ =	Velocity, 20 cm/sec 1.0	.5	.1	λ =	V = 40 cm/sec 1.0	.5
Fixed Σ_0 at 8.21×10^{-8} $D_0 = 5 \times 10^{-5}$									
Total	@ 1/2	24.07		24.25	24.21	24.13		24.21	24.16
	3/4	15.21		15.27	15.28	15.24		15.27	15.25
Leading	@ 1/2	10.62		10.58	10.59	10.61		10.59	10.60
	3/4	7.07		7.03	7.04	7.06		7.04	7.06
Trailing	@ 1/2	13.45		13.67	13.62	13.53		13.62	13.56
	3/4	8.13		8.27	8.23	8.18		8.23	8.19

Fixed at 1 sec^{-1}		Σ_0	5×10^{-8}	1.0×10^{-8}	$.5 \times 10^{-8}$
Total	@ 1/2		24.17	24.09	24.08
	3/4		15.27	15.22	15.22
Leading	@ 1/2		10.60	10.62	10.62
	3/4		7.05	7.07	7.08
Trailing	@ 1/2		13.57	13.47	13.46
	3/4		8.22	8.15	8.14

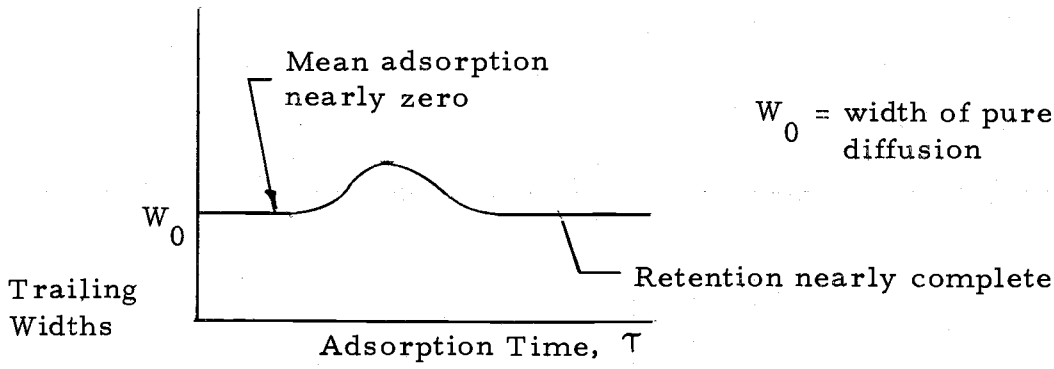

Figure 8. Trailing width versus adsorption time.

The bulk gas velocity, V, with respect to the column, has an effect on the gas packet that is inter-related with the adsorption time. In Figure 8 a specific adsorption, τ_{max}, exists that gives a maximum skewing of the packet. The τ_{max} is dependent directly on the gas velocity, as can be seen in Tables 5 and 6 by comparing the skewing as a function velocity. For a specific adsorption time, a relationship identical to that shown in Figure 8 exists but with adsorption time replaced by the bulk velocity, V. In Table 5 the velocity is past V_{max}, which is analogous to τ_{max}, that is the skewing is decreasing as the velocity increases, while in Table 6 the skewing is still increasing with V. Note that λ is 4 sec^{-1} in Table 6 while it is 1.0 and .5 sec^{-1} in Table 5.

Statistics

Six sets of data were taken and of them one set was decided upon for analysis. Each data set, which was defined as all the data

Table 6. Effect of velocity on packet skewing.

Widths		Velocity, cm/sec 0.0	10	20	30
Total	@ 1/2	24.013	24.055	24.140	24.201
	3/4	15.182	14.210	15.258	15.288
Leading	@ 1/2	10.600	10.547	10.533	10.533
	3/4	7.065	7.007	6.987	6.985
Trailing	@ 1/2	13.413	13.508	13.607	13.668
	3/4	8.117	8.203	8.271	8.303

Σ_0 = 1.0E-07
D_0 = 5.0E--5
λ = 4

taken on any specific day, contains one or more runs for the 40 cm and 270 cm columns. Two sets contained data that were acquired using one length column and were not used because of that. The other data sets were quite similar and the only reason one was chosen over the other was that it contained more runs with the 40 and 270 cm columns. The total widths of the chosen data set are shown in Table 7. Also shown are the mean widths and the RMS error associated with each width. The RMS error is defined by:

$$\overline{\Delta w}^2 = \frac{1}{N} \sum_{i}^{N} (w_i - \overline{w})^2$$

then

$$\text{RMS error} = \overline{\Delta w} \quad .$$

Where $\overline{w}$ is the mean width and N the number of runs in that

Table 7. Variation of width.

Total Width at:	40 cm Column		270 cm Column	
	1/2	3/4	1/2	3/4
	24.65	15.50	35.25	21.45
	23.35	14.80	34.40	21.10
	24.60	15.55	34.70	21.25
	22.90	14.95		
$\bar{w}$	23.90	15.20	34.80	21.25
Δw	.75	.34	.35	.25
% error	3%	2%	1%	.7%

Lapsed time between 40 and 270 cm was 9.5 sec
Velocity 24 cm/sec

data set. The RMS errors for both column lengths is 3% or less and for the 270 cm column they are 1% or less.

Data Fitting

To fit the profile of the 270 cm run with a code generated profile which started initially as the profile from a 40 cm run, required that the initial profile and the final profile should be consistant with the mean widths of Table 7. Profiles 2 and 1 of the 40 and 270 cm runs, respectively, were used for the initial and final profiles, after they were normalized so that their widths would closely match the mean widths. These runs were used because the ratio of their total widths at one-half and three-fourths the maximum peak height were closest to the ratio corresponding to the mean widths. Using these and matching the total widths at one-half maximum resulted in widths

that were within .5% of the mean widths.

In fitting the code generated profile to the exact profile, that is the one representing the experimental data, three variables had to be changed until a correct fit was established. In this analysis the values of D_0, Σ_0 and τ will be roughly found.

The first fit attempted was to find a value of the diffusion coefficient, D_0. In doing this the adsorption probability was set to zero and the initial profile was run with pure diffusion. In picking a diffusion coefficient that would be close to the correct one, the trailing and leading widths were compared to the final values so that the skewing that would take place when the Σ and λ were non-zero, would adjust the widths to their final values. In Table 8 the widths of four diffusion coefficients are compared with the exact widths. The total widths do not exceed those of the exact profile for any of the diffusion coefficients, but the leading widths do exceed the corresponding value of the exact profile between 10 and 12 x 10^{-5} cm^{-1} and 12 and 15 x 10^{-5} cm^{-1} for widths at one-half and three-fourths, respectively. Therefore, the value of diffusion coefficient must be at least larger than 12 x 10^{-5} cm, because with λ and Σ_0 non-zero the packet is skewed to such that the leading widths are less than the pure diffusion case. Therefore, the correct D_0 with Σ_0 and λ zero should produce leading edges larger than the exact profile's leading widths. Several other runs were made and

Table 8. Variation of diffusion coefficient.

Widths		WANT	10×10^{-5}	12×10^{-5}	15×10^{-5}	18×10^{-5}
Total	@1/2	34.77	30.47	31.59	33.13	34.50
	3/4	21.32	19.33	20.08	21.13	22.09
Leading	@1/2	13.99	13.79	14.17	15.16	15.54
	3/4	9.57	9.01	9.34	10.11	10.34
Trailing	@1/2	20.78	16.68	17.42	17.97	18.96
	3/4	11.74	10.19	10.74	11.02	11.74

14×10^{-5} cm^{-1} was found to produce the expected widths.

After finding a value of the diffusion coefficient that was reasonably close to the exact value, a series of runs with the code were made to establish a value of the adsorption time. During these runs the adsorption probability, Σ_0, was fixed at 10^{-7} cm^{-1} and the λ varied from 1 to 10 sec^{-1}. The maximum amount of skewing of the profile occurred at a value of about 2 sec^{-1}. With λ equal to λ_{max}, the amount of skewing was not enough to match the code generated widths with the exact widths, and increase in the adsorption probability, Σ_0, was needed. Varying of Σ_0, with $\lambda = 2$ sec^{-1}, from 10^{-7} cm^{-1} to 5×10^{-6} cm^{-1} was done. The results are in Table 9. The solution for Σ_0 at 5×10^{-6} did not converge to a reasonable answer. The widths corresponding to the values of D_0 from 10^{-7} to 10^{-6} were found to be quite linear. To find the value of the adsorption probability the leading and trailing widths were plotted and the values of Σ_0 corresponding to the exact

Table 9. Widths at three-fourths maximum for various values of Σ_0.

	Σ_0, cm^{-1}				
Width	Exact	0	10^{-7}	5×10^{-7}	10×10^{-7}
Total	21.32	20.79	20.98	21.10	21.27
Leading	9.57	10.02	10.00	9.81	9.60
Trailing	11.74	10.77	10.98	11.29	11.67

values of the widths were found by linear extrapolation. They both produced the exact results at 11.0×10^{-5} cm^{-1}. Below are the values found to produce a good agreement between those profiles produced by the computer code and those found by experiment.

$$D_0 = 14 \times 10^{-5} \text{ cm}$$

$$\lambda = 2 \text{ sec}^{-1}$$

$$\Sigma_0 = 11 \times 10^{-7} \text{ cm}^{-1}$$

The uncertainty associated with the values of the widths used to determine the above constant determines their uncertainty. The uncertainty associated with leading and trailing widths are small when compared to the total widths, but when compared to the changes in widths associated with Σ_0 yields values of the uncertainty in Σ_0 of nearly $\pm 2 \times 10^{-7}$ cm^{-1} or approximately 20%. When considering the uncertainty in the initial width the uncertainty is close to 50% in both λ and Σ_0 and 30% in D_0.

VI. CONCLUSION

Discussion of Data

With the evaluation of the constants required to fit the theoretical profile to the experimental profile, the validity of the model to the experimental system was checked. In checking the models validity, the concentration of adsorbed gas molecules was estimated, because for the model to be valid the adsorbed molecules must not approach a monomolecular layer.

With values of adsorption probability, the adsorption time, and an estimate of the collision density of the gas molecules with the column wall, the molecular wall concentration can be estimated. Assuming pure boron trifluoride gas at 1 atm and 20° C the collison density is:

$$\frac{4 \times 10^{23} \text{ collisions}}{\text{sec-cm}^2} .$$

The maximum molecular concentration, (i. e. a complete monomolecular layer), was calculated using 4.5×10^{-8} cm as the effective molecular diameter of the boron trifluoride molecule. The maximum concentration was 7.5×10^{13} molecules per cm of the column. With λ equal to 2 sec^{-1}, the equilibrium wall concentration, from equation (9) is:

$$C = 6.5 \times 10^{13} \text{ molecules per cm of column.}$$

The time constant associated with the approach to equilibrium can be estimated by solving equation (8), with the product of Z and P_0 equal to a constant. Doing this results in a time constant of 15.3 sec^{-1}. Such a large time constant indicates that the system is very close to an equilibrium condition at all times. With the system close to equilibrium, the wall concentration will be too close to a monomolecular layer for this model to apply rigorously. The large concentration on the column surfaces predicted by the model may indicate a large attraction between the boron trifluoride molecule and the teflon surface.

Above it was assumed that a large amount of adsorption had caused all of the skewing of the experimental profile, but another event may have caused some of the skewing. When the column was changed from 40 cm to 270 cm there may have been a change in flow rate that was too small for detection with the available instrumentation and methods. This small change in flow rate may have caused small changes in the initial profile, similar to those discussed in Chapter IV.

The major changes in the profiles occurred because of diffusion. The large changes in the profiles makes the value of the diffusion coefficient less sensitive to other perturbation in the system. Various methods have been developed to calculate the diffusion

coefficient. One method used is to calculate an effective molecular cross sectional area (23) and then calculate a probability of collision, Σ_c. With this macroscopic cross section, the diffusion coefficient can be calculated from:

$$D_0 = \frac{1}{(3\ \Sigma_c)} \cdot$$

Another method presented by Hirschfleder, Bird, and Sputz (17) for calculating a diffusion coefficient for a binary gas system using Lennard-Jones potentials can also be used for comparison with the experimental diffusion coefficient. Below are both comparisons in Table 10. The theoretical calculations are smaller than the experi-

Table 10. Comparison of theoretical and experimental diffusion coefficient.

Method	D_0
Experimental	14×10^{-5}
$\frac{1}{3\ \Sigma_c}$	3.5×10^{-5}
Hirschfelder	$.3 \times 10^{-5}$

mental value. The theoretical calculations do not agree among themselves any better than they do with the experimental values. Even though the experimental value is larger than what might be expected,

the theoretical calculations are not at a point of sophistication where they would be expected to be consistant.

Results

The mathematical model and the computer code used in this study were shown to be of value in gaining a better understanding of the physical mechanisms involved in capillary gas chromatography. The model is relatively simple and with the aid of today's modern high speed computers the solution to the model's equations was done quickly. The information obtained from the code calculations can be used to analyze experimental work to determine system parameters.

The hard-to-measure parameters associated with the adsorption-desorption process can be evaluated quickly with good chromatographic concentration profiles, and the aid of a computer. The diffusion coefficient for mixed gases used as carrier and sample gases in a gas chromatography can also be found.

Areas for Additional Work

In Chapter V it was mentioned that the solution of the two differential equations could be accomplished by expanding the concentration profiles with analytical functions. This would, if it could be done satisfactorily, be an important step in making the computer solution more useful. Now, the computer solution is limited because

convergence is strongly dependent on both, the sizes and the relative sizes of the space and time divisions. By using analytical functions to describe the profiles as a function of space, only the time division should effect convergence.

A limited form of BET theory could be included into the model. If only a second molecular layer could be included in the model, it would be much more useful.

The experimental system could be improved with a gas flow control system that could regulate the carrier gas flow rate to a constant value. The gas detector, an important part of the system, should be designed so that the concentration magnitude could also be used, instead of only the profile shape. It may have been only the specific detector that was used in which the problem of fluxation of concentration magnitude was present.

The separations of isotopes has been an interest in the nuclear field since its conception. The economic separation of specific isotopes is recognized as an important problem in the nuclear industry. Chromatographs have been used as early as 1938 (25) in an attempt to separate isotopes. The isotopes of lithium have been separated by many workers (25, 12, 13) using liquid chromatography. Gas chromatography has been used to separate the isotopes of neon (12, 2), oxygen (3) and nitrogen (7).

A superb structural material for nuclear reactors would result

if titanium could be enriched in its low neutron capture cross-section isotopes. It may even be possible to separate the isotopes of heavy elements like uranium with capillary gas chromatography. More work in the field of heavy isotope separation with gas chromatography would no doubt benefit the nuclear industries.

BIBLIOGRAPHY

1. Adamson, A. W. Physical chemistry of surfaces. 2d ed. New York, Interscience Publishers, 1967. 747 p.

2. Blanc, C., C. Huynh and L. Espagno. Enrichissement des isotope du cardone et du neon par chromatographic en phase gazense. Journal of Chromatography 28:194-208. 1967.

3. Bocola, W., F. Bruner and G. P. Cartoni. Separation of oxygen isotopes by gas chromatography. Nature 209:200-201. 1966.

4. Bosanquet, C. H. The diffusion at a front in gas chromatography. In: Gas chromatography, ed. by D. H. Desty. London, Butterworths Publications Ltd. 1958. p. 107-115.

5. Brunauer, S., L. E. Copeland and D. L. Kantro. The Langmuir and BET theory. In: The solid-gas interface, ed. by E. A. Flood. New York, Marcel Dekker Inc., 1967. p. 77-103.

6. Brunauer, S., P. H. Emmett and E. Teller. Adsorption of gases in multimolecular layers. Journal of American Chemical Society 60:309. 1938.

7. Cartoni, G. P. and M. Passanzini. The separation of nitrogen isotopes by gas chromatography. Journal of Chromatography 30:99-100. 1969.

8. Dal Nogere, S. and R. S. Juvet, Jr. Gas liquid chromatography. New York, Interscience Publishers, 1962. 450 p.

9. De Boer, H. The dynamical characters of adsorption. Oxford, The Clarendon Press, 1963. 400 p.

10. De Vault, D. The theory of chromatography. Journal of American Chemical Society 1943:297-301. 1943.

11. Frenkle, Y. I. Kinetic theory of liquid. London, Dover Publications, 1955.

12. Gluechanf, E., K. H. Barker and G. P. Kitt. The separations of lithium isotopes by ion exchange and of neon isotopes by low-temperature adsorption columns. Discussion of the Faraday Society 7:199-213. 1949.

13. Gross, J. H. The enrichment of lithium isotopes by ion-exchange. 1950. 3 p. (U. S. Atomic Energy Commission. AECD-2952) (Microcard)

14. Habgood, H. W. Chromatography and the solid-gas interface. In: The solid gas interface, ed. by E. Alison Flood. New York, Marcel Dekker, Inc. 1967. p. 611-646.

15. Heftmann, E. Chromatography. New York Reinhold Publishing Corp., 1962. 450 p.

16. Hilderbrand, F. B. Introduction of numerical analysis. New York, McGraw-Hill Book Co., 1956. 507 p.

17. Hirschfelder, J. O., R. B. Bird and E. L. Spotz. The transport properties of gases an gases in gaseous mixtures. Chemical Reviews 44:205-231. 1949.

18. James, A. T. and A. J. P. Martin. Gas-liquid parition chromatography. Journal of Biochemistry 50:679-690. 1952.

19. Kiseley, A. V. and D. P. Poshkus. Statistical calculation of thermodynamic functions of an adsorbed substance on graphite. Transaction Faraday Society 59:176-191. 1963.

20. Krige, G. J. and V. Pretorins. Frontal analysis chromatography. Analytical Chemistry 37:1186-1202. 1965.

21. Langmuir, I. The adsorption of gases on plane surfaces of glass, mica and platinum. Journal of American Chemical Society 40:1361-1373. 1918.

22. Martin, A. J. P. and R. L. M. Synge. A new form of chromatogram employing two liquid phases. Journal of Biochemistry 35:1358-1368. 1941.

23. Moore, J. J. Physical chemistry. 3d ed. New Jersey, Prentice-Hall Inc., 1964. 844 p.

24. Polland, F. H. and C. J. Hardy. A preliminary study of some factors influencing the order of elution of halogenated methanes, the degree of separation, and the reproducibility of retention volumes in gas-liquid partition chromatography. In: Vapour phase chromatography, ed. by D. H. Desty. London, Butterworth Publications Ltd. p. 115-126. 1957.

25. Taylor, T. I. and H. C. Urey. Fractionation of the lithium and potassium isotopes by chemical exchanges with zeolites. Journal of Chemical Physics 6:429-438. 1938.

26. Welty, J. R., C. E. Wicks and R. E. Wilson. Fundamental of momentum, heat and mass transfer. New York, John Wiley and Sons, Inc., 1969. 697 p.

27. Wiese, J. On the theory of chromatography. Journal of the Chemical Society. 1943:297-303. 1943.

28. Wilson, J. H. A theory of chromatography. Journal of the American Chemical Society 62:1583-1591. 1940.

APPENDIX

APPENDIX A

Solution to the Integral Transport Equation

The problem is to find the number of collisions the gas molecules make with the surface of the wall per second per unit area in an infinitely long cylinder. The assumptions made are:

1. All collision between gas molecules are isotropic in the lab frame of reference,
2. The gas is monoenergetic, and
3. The gas density, n, is constant.

Next step is to define a coordinate system that will fit the problem. Let $\bar{r}$ be the position vector of our coordinates system, whose origin is located on the surface, at O, of the cylinder. Let ϕ and θ be defined as in Figure 9. Now let n and v be the molecular density of the gas and the average molecular velocity, respectively. D is the cylinder diameter.

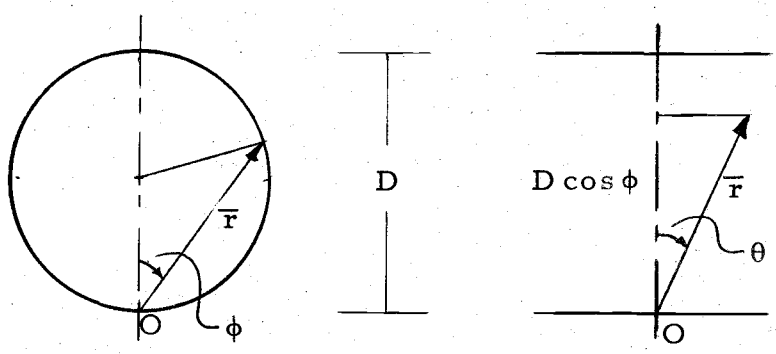

Figure 9. Coordinate system for solution of integral transport equation.

The integral is constructed using the point attenuation kernal,

$$K(r) = \frac{\exp(-\Sigma r)}{4\pi r^2} ,$$

which has built-in the assumptions one and two. Where Σ is the inverse of the mean free path length of the gas.

The number of collision per second per unit area, Z, is

$$Z = \int_{vol} \Sigma K(r) nv \, dV .$$

The volume element, dV, is produced by determining the differential area of volume element normal to r and then multiplying it by the differential thickness, dr. The differential area is found by allowing differential variation in the angles ϕ and θ.

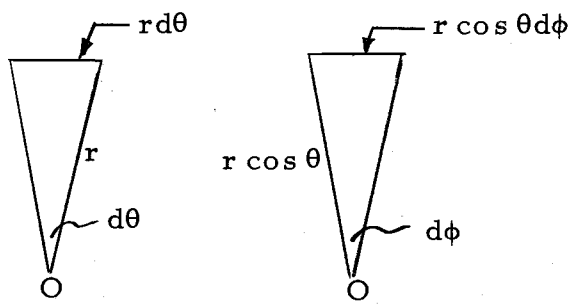

$$dA = (r\,d\theta) \times (r\cos\theta\, d\phi) = r^2 \cos\theta\, d\phi\, d\theta$$

$$dV = (dr) \times (dA) = r^2 \cos\theta\, d\phi\, d\theta\, dr$$

Figure 10. Volume element construction.

The volume element is constructed in Figure 10 and the integral is:

$$Z = \int_{vol} \Sigma nv \frac{\exp(-\Sigma r)}{4\pi r^2} r^2 \cos\theta d\phi\, d\theta dr .$$

The limits on the integral are for:

$$r: \ 0 \text{ to } D\frac{\cos\phi}{\cos\theta}$$

$$\theta: \ -\frac{\pi}{2} \text{ to } \frac{\pi}{2}$$

$$\phi: \ -\frac{\pi}{2} \text{ to } \frac{\pi}{2} .$$

Now:

$$Z = \int_{-\frac{\pi}{2}}^{\frac{\pi}{2}} \int_{-\frac{\pi}{2}}^{\frac{\pi}{2}} \int_{0}^{D\frac{\cos\phi}{\cos\theta}} \frac{\Sigma \, Vn}{4\pi r^2} \exp(\Sigma r) \, r^2 \, dr \, d\phi \, d\theta .$$

$$Z = \frac{\Sigma n}{\pi} \int_{0}^{\frac{\pi}{2}} \int_{0}^{\frac{\pi}{2}} \int_{0}^{D\frac{\cos\phi}{\cos\theta}} \cos\theta \exp(\Sigma r) \, dr \, d\phi \, d\theta .$$

The r integration can be carried on exactly,

$$Z = \frac{nv}{\pi} \int_{0}^{\frac{\pi}{2}} \int_{0}^{\frac{\pi}{2}} \cos\theta \left(1 - \exp\left(- D\Sigma \frac{\cos\phi}{\cos\theta}\right)\right) d\theta \, d\phi .$$

Two integrals are left, with the cosine term integration carried out the integral is

$$Z = \frac{vn}{\pi} \left(\frac{\pi}{2} - \Psi(D, \Sigma)\right)$$

where

$$\Psi(D, \Sigma) = \int_{0}^{\frac{\pi}{2}} \int_{0}^{\frac{\pi}{2}} \cos\theta \exp\left(- D\Sigma \frac{\cos\phi}{\cos\theta}\right) d\phi \, d\theta .$$

The Ψ term must be evaluated numerically.

The numerical integration was done with Σ equal to $6.25 \times 10^4 cm^{-1}$ and D equal to .0381 cm. The numerical scheme was a two dimensional trapizoid integrations using

$$\int_0^a \int_0^b f(x, y)\, dxdy = \left(\frac{\Delta x \Delta y}{4}\right) \sum_i \sum_j f(x_i, y_j)\, a_{ij} .$$

Where a_{ij} is the matrix elements of the matrix A which gives the weighting coefficient for trapizoid integration with even spacings.

$$A = \begin{pmatrix} 1 & 2 & 2 & . & . & . & 1 \\ 2 & 4 & 4 & . & . & . & 2 \\ 2 & 4 & 4 & . & . & . & 2 \\ . & . & . & . & & & . \\ . & . & . & & . & & . \\ . & . & . & & & . & . \\ 1 & 2 & 2 & . & . & . & 1 \end{pmatrix}$$

The result of the numerical integration produce

$$\Psi\,(.0381,\ 6.25 \times 10^{4}) = .00618$$

which is only less than .4% of the total integral.

APPENDIX B

Computer Code GAS CHROMATOGRAPHY

Abstract

The code was written to solve the two basic one-dimensional time dependent differential equations describing the diffusion and adsorption-description processes occurring to a sample gas packet in a capillary column of a gas chromatograph. The diffusion is described by simple diffusion theory and the adsorption process uses Langmuir theory. The equations are:

$$\frac{dN(x)}{dt} = D \frac{d^2}{dx^2} N(x) - \Sigma N(x) + \lambda C(x')$$

and

$$\frac{dC(x')}{dt} = \Sigma N(x) - \lambda C(x') \qquad x' = x = vt \ .$$

Where

C = molecular concentration of the column walls.

N = gas density.

Σ = adsorption probability.

λ = inverse of adsorption time.

D = diffusion coefficient.

The solution uses a simple step by step integration to find the

final concentration profile. The program is written in subroutine form and inputs are of the TTYIN type. The TTYIN inputs of the Oregon State University's OS3 computer system are for remote terminal use only.

PRØGRAM GAS CHRØATØGRAPHY

```
 FILE  *GAS

       CØMMØN ML,PER,CØ,DC,HT,H,IT,DL,XA,GV,NL,DF(200)
C-------------------------------------------------------------
C      READ IN DATA
C-------------------------------------------------------------
       H=TTYIN(4HHX= )      $    HT=TTYIN(4HHT= )
       TD=TTYIN(4HTD= )     $    DC=TTYIN(4HD CØ,4HNST=)
       DL=TTYIN(4HDECA,4HY CØ,4HNST=)
       IF(DL .EQ. 0) GØ TØ 1
       XA=TTYIN(4HXA= )     $    ML=TTYIN(4HML= )
       CØ=TTYIN(4HCØ= )     $    NL=TTYIN(4HNL= )
       PER=TTYIN(4HFRAC,4HTIØN,4H EQ=)
1      MW=TTYIN(4HMW= )     $    TEMP=TTYIN(4HTEMP,3H=  )
       GV=1.455E04*SQRT((TEMP+273.3)/MW)
       IT=TD/HT             $    I=IT+1
C-------------------------------------------------------------
C      CALL SUBRØUTINES
C-------------------------------------------------------------
       CALL INITIAL
       GØ TØ(3,2)I
2      CALL DIFFUSE
3      CALL SHAPE
C-------------------------------------------------------------
C      PRINT ØUT PACKET SHAPES
C-------------------------------------------------------------
       PRINT 102            $    I=TTYIN(4HI=  )
       IF(I.NE. 1) GØ TØ 40
       I=TTYIN(4HFRAC,4HTIØN,4H= 1/)
       WRITE(31,101)
       DØ 4 J=I,100,I       $    K=J+100
4      WRITE(31,100)J,DF(J),K,DF(K)
40     CØNTINUE
100    FØRMAT(2(3X,I3,4X,F10.4,7X))
101    FØRMAT(2(2X,'INDEX',6X,'HIEGTH',8X))
102    FØRMAT(' FØR PRINT ØUT, I=1')
       END
```

```
                    SUBRØUTINE INITIAL
 FILE  *INITIAL

      REAL L1,L2,L3
      DIMENSIØN D(2,40)
      CØMMØN I8,E1,E2,E3,E4,H,I7,E6,E7,E8,I9,DF(200)
C-----------------------------------------------------------------
C     READ DATA FØR INITIAL SHAPE AND CALC. MISC. CØNSTANTS
C-----------------------------------------------------------------
      PRINT 102
      REWIND 30        $   READ(30,100) IDP
      READ(30,101)(D(1,I),D(2,I),I=1,IDP)
      WIDTH=D(1,IDP)-D(1,1)
      FWIDTH=200*H     $   IFIRST=(FWIDTH-WIDTH)/(2*H)
      A0=D(1,1)        $   J=IFIRST       $   K=3
      D0 1 I=1,IDP
1     D(1,I)=D(1,I)-A0
C-----------------------------------------------------------------
C     CALC. LAGRANGAIN C0EFFICIENTS AND INTERP0LATE
C-----------------------------------------------------------------
2     D0 4 I=K,IDP,2
      A0=D(2,I-2)/((D(1,I-2)-D(1,I-1))*(D(1,I-2)-D(1,I)))
      A1=D(2,I-1)/((D(1,I-1)-D(1,I-2))*(D(1,I-1)-D(1,I)))
      A2=D(2,I)/((D(1,I)-D(1,I-2))*(D(1,I)-D(1,I-1)))
      L1=A0+A1+A2
      L2=-(A1+A2)*D(1,I-2)-(A0+A2)*D(1,I-1)-(A0+A1)*D(1,I)
      L3=D(1,I-1)*(A0*D(1,I)+A2*D(1,I-2))+D(1,I-2)*D(1,I)*A1
3     X=H*(J-IFIRST)
      IF(X.GT.D(1,I)) G0 T0 4
      DF(J)=L3+(L2+L1*X)*X
      J=J+1            $   G0 T0 3
4     C0NTINUE
      IF(2*((IDP-1)/2)+1.LT.IDP.AND.K.DQ.3)5,6
5     K=IDP            $   G0 T0 2
6     C0NTINUE
100   F0RMAT(I2)
101   F0RMAT(2F10.4)
C-----------------------------------------------------------------
102   F0RMAT(' INITIAL')
      END
```

SUBRØUTINE DIFFUSE

```
 FILE  *DIFF

       CØMMØN ML,PER,CØ,DC,HT,H,IT,DL,XA,GV,NL,DF(200),C(200)
       PRINT 101
       DHH=HT*GV*DC/(H*H)
       IF(DL .EQ.0 .ØR. XA.EQ.0) GØ TØ 10
C      DIFFUSIØN WITH WALL ADSØR. AND DESØR.  ******************
       C2=GV*XA   $   IT=IT/ML
       DØ 3 I=1,199 $ C1=C2*DF(I)
3      C(I)=C1*PER/(DL+C1/CØ)
       C1=HT*XA*GV $ C2=(1-EXP(-HT*DL))
       DØ 8 I=1,IT
       DØ 5 I1=1,ML  $A=0
       DØ 5 J=2,199 $ DELL=(DF(J+1)-2*DF(J)+A)*DHH $ A=DF(J)
       DF(J)=DF(J)+DELL-C1*(1-C(J)/CØ)*DF(J)+C2*C(J) $B1=C(J)
       C(J)=C(J)+C1*(1-C(J)/CØ)*DF(J)-C2*C(J)
       IF(DF(J).GT. 1.0E-200) GØ TØ 5 $ DF(J)=C(J)=0
5      CØNTINUE $ J1=200-NL
       DØ 6 J=1,J1 $ K=201-J $ M=K-NL
6      C(K)=C(M) $ J1=J1+1
       DØ 7 J=J1,199 $ K=201-J
7      C(K)=0
8      CØNTINUE
       RETURN
C       PURE DIFFUSIØN  ******************************************
10     DØ 20 I=1,IT $ A=0
       DØ 20 J=2,199
       DELL=(DF(J+1)-2*DF(J)+A)*DHH $ A=DF(J)
       DF(J)=DF(J)+DELL
       IF(DF(J).LT. 1.0E-200) DF(J)= 0.0
20     CØNTINUE
        RETURN
101    FØRMAT(' DIFFUSE')
       END
```

SUBRØUTINE SHAPE

FILE *SHAPE

```
      DIMENSIØN X(2,2)
      CØMMØN ML,PER,CØ,DC,HT,H,IT,DL,XA,GV,NL,DF(200)
      PRINT 104      $   AMAX=0
      Dø 1 I=1,200
      IF(DF(I) .LT. AMAX) GØ TØ 1 $ AMAX=DF(I) $ IMAX=I
1     CØNTINUE $ AMAX=AMAX/100.0
      DØ 2 I=1,200
2     DF(I)=DF(I)/AMAX $ A=50
      DØ 6 J=1,2 $J1=1
      DØ 5 I=1,200
      IF(DF(I) .LT. A .AND. DF(I+1) .GT. A) GØ TØ 4
      IF(DF(I) .GT. A .AND. DF(I+1) .LT. A) 3,5
3     J1=2
4     C1=H/(DF(I+1)-DF(I)) $ B= H*I-C1*DF(I)
      X(J1,J)=B+C1*A
5     CØNTINUE
6     A=75 $ C1=IMAX*H
      DØ 7 I=1,2 $ DØ 7 J=1,2
7     X(J,I)=ABS(C1-X(J,I))
      FW1=X(1,1)+X(2,1) $ FW3=X(1,2)+X(2,2)
      PRINT 100,FW1,FW3
      PRINT 101,X(1,1),X(2,1),X(1,2),X(2,2)
      PRINT 102,AMAX
      RETURN
100   FØRMAT(//' FW AT: 1/2',F12.3,//7X,' 3/4',F12.3)
101   FØRMAT(//6X,' EDGE:',7X,'LEADING',10X,'TRAILING',//
     1' WIDTH:  1/2',7X,F7.3,11X,F7.3,//,8X,' 3/4',7X,F7.3,
     211X,F7.3)
102   FØRMAT(//,' PEAK DRØP BY  ',F10.4,//)
104   FØRMAT(' SHAPE')
      END
```

APPENDIX C

Program DATAPR

Abstract

The data taken from the gas chromatograph's recorder charts are preliminarily processed by the code DATAPR. The code converts the data, which was a function of the chart position, to a function of both time and physical position, normalizes concentration peak values to values to 100. The code also keeps a running integral at each point.

The width of the peak, total, leading and trailing are also calculated. The code inputs are designed for reading computer stored data in the OSU's OS3 system.

PRØGRAM DATAPRØCESSING

```
 FILE  DATAPR

       DIMENSIØN P(4,40),B(80),D(2,40),X(2)
2      READ(30,98)(B(I),I=1,80)
       IF(EØFCKF(30).EQ.1) GØ TØ 1
       READ(30,99)IDP,SP,CL
       READ(30,100)(D(1,I),D(2,I),I=1,IDP)
       F=D(1,1) $ F1=D(2,1) $ F2=0
       DØ 10 I=1,IDP
       P(1,I)=SP*(D(1,I)-F) $ P(2,I)=D(2,I)-F1
       IF(P(2,I).GT.F2)9,10
9      F2=P(2,I) $ TP=P(1,I)
10     CØNTINUE
       GV=CL/TP
       DØ 11 I=1,IDP
11     P(2,I)=100*P(2,I)/F2
       P(3,1)=0
       DØ 12 I=2,IDP
       H=P(1,I)-P(1,I-1)
12     P(3,I)=P(3,I-1)+(P(2,I)+P(2,I-1))*GV*H/2.0
       DØ 13 I=1,IDP
13     P(4,I)=P(1,I)*GV
       X(1)=X(2)=0$ A=50
       DØ 26 J=1,2 $ J1=0
       DØ 25 I=1,IDP
       IF(P(2,I).LT.A.AND.P(2,I+1).GT.A) 24,22
22     IF(P(2,I).GT.A.@ND.P(2,I+1).LT.A) 23,25
23     J1=1
24     C=(P(4,I+1)-P(4,I))/(P(2,I+1)-P(2,I))
       B=P(4,I)-C*P(2,I)
       X(J)=B+C*A-X(J) $ IF(J1.EQ.1)26,25
25     CØNTINUE
26     A=75
       WRITE(61,97)(B(I),I=1,80)
       WRITE(61,105)X(1),X(2)
       WRITE(61,101) GV $ WRITE(61,102)
       WRITE(61,103)((P(J,I),J=1,4),I=1,IDP)
       I=(54-IDP)/2.0
       DØ 14 J=1,I
14     WRITE(61,104)
       GØ TØ 2
97     FØRMAT(///,2X,80A1)
98     FØRMAT(1X,80A1)
99     FØRMAT(I2,2(/F13.5))
100    FØRMAT(2(F10.5))
101    FØRMAT(//,' GAS VØLØCITY',F13.4)
102    FØRMAT(///,8X,' TIME',10X,' HEIGHT',10X,' INTEGRAL',
      110X,' PØSITIØN')
103    FØRMAT(2X,F13.4,3X,F13.4,5X,E13.4,7X,F13.4)
104    FØRMAT(/)
105    FØRMAT(//' WIDTHS:  1/2',F13.3,' CM.',/10X,'3/4',F13.3)
1      CØNTINUE
       END
```

PRØGRAM DATAPRØCESSING

```
 FILE  DATAPR

      DIMENSIØN P(4,40),B(80),D(2,40),X(2)
2     READ(30,98)(B(I),I=1,80)
      IF(EØFCKF(30).EQ.1) GØ TØ 1
      READ(30,99)IDP,SP,CL
      READ(30,100)(D(1,I),D(2,I),I=1,IDP)
      F=D(1,1) $ F1=D(2,1) $ F2=0
      DØ 10 I=1,IDP
      P(1,I)=SP*(D(1,I)-F) $ P(2,I)=D(2,I)-F1
      IF(P(2,I).GT.F2)9,10
9     F2=P(2,I) $ TP=P(1,I)
10    CØNTINUE
      GV=CL/TP
      DØ 11 I=1,IDP
11    P(2,I)=100*P(2,I)/F2
      P(3,1)=0
      DØ 12 I=2,IDP
      H=P(1,I)-P(1,I-1)
12    P(3,I)=P(3,I-1)+(P(2,I)+P(2,I-1))*GV*H/2.0
      DØ 13 I=1,IDP
13    P(4,I)=P(1,I)*GV
      X(1)=X(2)=0$ A=50
      DØ 26 J=1,2 $ J1=0
      DØ 25 I=1,IDP
      IF(P(2,I).LT.A.AND.P(2,I+1).GT.A) 24,22
22    IF(P(2,I).GT.A.@ND.P(2,I+1).LT.A) 23,25
23    J1=1
24    C=(P(4,I+1)-P(4,I))/(P(2,I+1)-P(2,I))
      B=P(4,I)-C*P(2,I)
      X(J)=B+C*A-X(J) $ IF(J1.EQ.1)26,25
25    CØNTINUE
26    A=75
      WRITE(61,97)(B(I),I=1,80)
      WRITE(61,105)X(1),X(2)
      WRITE(61,101) GV $ WRITE(61,102)
      WRITE(61,103)((P(J,I),J=1,4),I=1,IDP)
      I=(54-IDP)/2.0
      DØ 14 J=1,I
14    WRITE(61,104)
      GØ TØ 2
97    FØRMAT(///,2X,80A1)
98    FØRMAT(1X,80A1)
99    FØRMAT(I2,2(/F13.5))
100   FØRMAT(2(F10.5))
101   FØRMAT(//,' GAS VØL0CITY',F13.4)
102   FØRMAT(///,8X,' TIME',10X,' HEIGHT',10X,' INTEGRAL',
     110X,' PØSITIØN')
103   FØRMAT(2X,F13.4,3X,F13.4,5X,E13.4,7X,F13.4)
104   FØRMAT(/)
105   FØRMAT(//' WIDTHS:  1/2',F13.3,' CM.',/10X,'3/4',F13.3)
1     CØNTINUE
      END
```

APPENDIX D

Experimental Data Used for Analysis

Run #1		Run #2		Run #3		Run #4	
Position	Height	Position	Height	Position	Height	Position	Height
0	0	0	0	0	0	0	0
2.5000	8.7227	1.2500	2.4038	3.0000	11.4458	1.5000	4.7319
5.0000	24.9221	3.7500	11.5385	5.5000	27.7108	4.0000	15.7729
7.5000	45.1713	6.2500	27.4038	8.0000	48.1928	6.5000	32.8076
10.0000	65.7321	8.7500	46.1538	10.5000	66.2651	9.0000	53.6278
12.5000	81.9315	11.2500	67.3077	13.0000	83.7349	11.5000	73.5016
13.7500	88.7850	13.7500	84.1346	14.2500	89.7590	12.7500	82.0189
15.0000	93.7695	15.0000	90.8654	15.5000	93.9759	14.0000	89.2744
16.2500	97.5078	16.2500	95.1923	18.0000	98.1928	15.2500	94.3218
17.5000	99.3769	18.7500	99.5192	19.2500	100.0000	16.5000	98.1073
18.5000	100.0000	19.7500	100.0000	20.5000	98.1928	19.0000	100.0000
20.0000	99.3769	21.2500	98.0769	21.7500	96.3855	20.2500	99.0536
21.2500	96.2617	23.7500	90.8654	23.0000	92.1687	21.5000	96.2145
22.5000	92.5234	26.2500	79.8077	25.5000	83.7349	24.0000	86.7508
25.0000	83.4891	28.7500	67.3077	28.0000	71.6867	26.5000	75.7098
27.5000	72.5857	31.2500	55.7692	30.5000	59.6386	29.0000	64.6688
30.0000	61.3707	33.7500	44.7115	33.0000	49.3976	31.5000	49.8423
32.5000	50.7788	36.2500	36.0577	35.5000	40.9639	34.0000	38.8013
35.0000	41.7445	38.7500	29.3269	40.5000	27.1084	36.5000	31.5457
37.5000	34.2679	43.7500	19.2308	45.5000	17.4699	29.0000	26.1830
40.0000	27.4143	51.2500	11.0577	55.5000	10.8434	44,0000	17.9811

APPENDIX D (continued)

Run #1		Run #2		Run #3		Run #4	
Position	Height	Position	Height	Position	Height	Position	Height
42.5000	23.0530	63.7500	5.7692	73.0000	5.4217	49.0000	13.5647
45.0000	19.6262	76.2500	3.8462	85.5000	4.2169	61.5000	7.8864
50.0000	13.3956	88.7500	2.8846			74.0000	5.3628
57.5000	9.0343					86.5000	4.1009
67.5000	6.2305						
75.0000	4.6729						
87.5000	4.0498						

Date May 12th
Gas Velocity, V - 24.5 cm/sec
Temperature 20° C
Column Length 40 cm

APPENDIX D (continued)

Run #1		Run #2		Run #3	
Position	Height	Position	Height	Position	Height
0	0	0	0	0	0
2.5000	4.0741	2.5000	2.0067	2.5000	1.9506
5.0000	8.1481	5.0000	5.3512	5.0000	5.9818
7.5000	15.5556	7.5000	12.0401	7.5000	13.7841
10.0000	27.4074	10.0000	21.7391	10.0000	24.8375
12.5000	40.3704	12.5000	33.4448	12.5000	40.4421
15.0000	55.5556	15.0000	48.1605	15.0000	56.6970
17.5000	69.6296	17.5000	61.8729	17.5000	72.3017
20.0000	81.4815	20.0000	75.2508	20.0000	85.3056
22.5000	91.4815	22.5000	86.9565	22.5000	94.5384
25.0000	97.0370	25.0000	94.6488	23.7500	97.6593
27.5000	99.6296	26.2500	97.3244	25.0000	99.3498
28.5000	100.0000	27.5000	98.9967	27.0000	100.0000
30.0000	99.2593	30.0000	100.0000	28.7500	98.9597
32.5000	96.2963	31.2500	99.3311	30.0000	96.4889
35.0000	89.6296	32.5000	97.6589	32.5000	90.5072
37.5000	82.9630	35.0000	92.9766	35.0000	82.1847
40.0000	75.1852	37.5000	86.2876	37.5000	72.9519
42.5000	67.4074	40.0000	78.5953	40.0000	63.3290
47.5000	53.7037	42.5000	70.2341	42.5000	53.8362
52.5000	43.7037	45.0000	62.8763	45.0000	45.7737
57.5000	34.8148	47.5000	54.1806	47.5000	38.7516
62.5000	30.0000	50.0000	49.4983	50.0000	32.6398
72.5000	23.7037	52.5000	43.4783	52.5000	27.5683

APPENDIX D (continued)

Run #1		Run #2		Run #3	
Position	Height	Position	Height	Position	Height
82.5000	19.2593	57.5000	33.7793	55.0000	23.5371
100.0000	15.1852	62.5000	27.7592	57.5000	20.2861
112.5000	12.9630	72.5000	20.4013	62.5000	15.3446
		90.0000	14.7157	67.5000	12.4837
		102.5000	12.7090	72.5000	10.4031
		127.5000	10.0334	82.5000	7.8023
				95.0000	6.1118
				107.5000	5.2016

Date May 12th
Gas Velocity, V = 24.5 cm/sec
Temperature 20° C
Column Length 270 cm